JOURNAL OF VIROLOGY, Nov. 1994, p. 7083–7091
0022-538X/94/$04.00+0

Vol. 68, No. 11

PCR-Based Analysis of Herpes Simplex Virus Type 1 Latency in the Rat Trigeminal Ganglion Established with a Ribonucleotide Reductase-Deficient Mutant

RAMESH RAMAKRISHNAN,[1] MYRON LEVINE,[1]* AND DAVID J. FINK[2]

Department of Human Genetics[1] and Department of Neurology and VA Medical Center,[2] University of Michigan Medical School, Ann Arbor, Michigan 48109-0618

Received 23 May 1994/Accepted 3 August 1994

Competitive quantitative PCR and reverse transcriptase-PCR were used to quantitate DNA and RNA from an attenuated ribonucleotide reductase-deleted herpes simplex virus type 1 (HSV-1) mutant in the rat trigeminal ganglion after peripheral inoculation following corneal scarification. Amplification of ganglionic DNA with oligonucleotide primers specific for the HSV-1 glycoprotein B (*gB*) gene and for the latency-associated transcript (*LAT*) gene indicated that there were approximately 2×10^5 genome equivalents per ganglion at 2 days, 7 days, and 8 weeks after inoculation. Amplification of ganglionic RNA with primers specific for HSV-1 LAT indicated that the amount of LAT RNA was also stable over 8 weeks, with 10^7 LAT molecules per ganglion at 2 days and at 7 days postinoculation and 1.4×10^7 LAT molecules per ganglion at 8 weeks. In situ hybridization with a digoxigenin-labeled riboprobe specific for LAT detected an average of one to two LAT-positive cells in each positive 6-μm section of trigeminal ganglion. In situ PCR detection of HSV-1 genomes in similar sections, using digoxigenin-labeled nucleotides with primers specific for HSV-1 *gB*, identified as many as 120 genome-positive cells per section. These results indicate that there are approximately 50 LAT molecules per latent HSV-1 genome in the trigeminal ganglion, compared with 15 LAT molecules per latent HSV-1 genome in the central nervous system (R. Ramakrishnan, D. J. Fink, G. Jiang, P. Desai, J. C. Glorioso, and M. Levine, J. Virol. 68:1864–1873, 1994), but that cells with detectable LATs by in situ hybridization represent only a small proportion of those ganglionic neurons containing HSV-1 genomes. The presence of latent HSV-1 genomes in a large number of neurons suggests that HSV-1 may be more efficient in establishing the latent state than would be anticipated from previous reports.

A characteristic feature of infection with herpes simplex virus type 1 (HSV-1) is the capacity of the virus to establish life-long latency in the nervous system of the host (14, 19, 34, 40). In the course of infection of the skin or mucosal surfaces, virus is taken up by axon terminals and transported to the nuclei of neuronal cell bodies in sensory ganglia, where after a short phase of active replication (41), viral genomes persist in a circular or concatameric form (12, 26, 31) with a chromatin-like organization (9). Expression of the more than 70 genes of HSV-1 is repressed in the latent state (18, 40), and only the loci of the viral genes coding for the latency-associated transcripts (LATs) are active. LATs are transcribed from the strand opposite to that of the *ICP0* gene in the inverted repeat sequence of the long unique (U_L) segment of the viral genome and are partially complementary to ICP0 mRNA (7, 29, 32, 42, 43). A 2-kb LAT is the most abundant species, with smaller amounts of 1.5- and 1.45-kb coterminal molecules also found in latently infected ganglia (7, 27, 37, 43, 44, 45). These RNAs are intranuclear and not polyadenylated (11, 37, 44). No protein product has been associated with the LAT locus, and no function for the LATs has been defined. Virus mutants which do not transcribe LAT RNA are nonetheless able to establish and maintain latency (19, 36, 39), although some of these mutants are defective in reactivation from latency (3, 10, 22).

* Corresponding author. Mailing address: Department of Human Genetics, University of Michigan, Ann Arbor, MI 48109-0618. Phone: (313) 764-1356. Fax: (313) 763-3784.

We have previously reported the results of a quantitative study characterizing the establishment of HSV-1 latency in the rat brain following stereotactic intracranial inoculation of a highly attenuated mutant into the hippocampal region (30). The infecting virus was deleted for the coding sequence of both ribonucleotide reductase (RR) subunit genes, U_L39 (RR1) and U_L40 (RR2). Using DNA and RNA competitive quantitative PCR, we demonstrated a large number of latent viral genomes (8×10^4) and LAT RNA molecules (1.2×10^6) in tissue scaped from isolated regions of single 10-μm brain sections. The number of viral genomes and the number of LAT molecules remained constant up to 8 weeks postinoculation (p.i.); there were approximately 15 molecules of LAT for each HSV-1 genome during latency.

To compare latency in the central nervous system, established by direct intracranial inoculation of virus, with the natural latent state in the peripheral nervous system, we have used the same HSV-1 mutant and competitive quantitative PCR and reverse transcriptase-PCR (RT-PCR) techniques to determine the number of viral genomes and LAT RNA molecules in the trigeminal ganglion of the rat, after achieving infection by corneal scarification and inoculation of virus. We have combined these quantitative measurements with in situ hybridization to determine the number of LAT (RNA)-positive cells in the ganglia and in situ PCR to define the cells harboring viral genomes (DNA) in the same ganglia. We find that there are a large number of neurons containing viral genomes in the trigeminal ganglion but that only a small fraction of these genome-harboring neurons express detectable LATs.

MATERIALS AND METHODS

Cells and viruses. All experiments reported were done with a virus designated RR1*CAT*/RR2*lacZ* (8), an RR-deleted derivative of HSV-1 KOS in which the RR1 promoter drives chloramphenicol acetyltransferase expression and the RR2 promoter drives expression of β-galactosidase. HSV-1 strains mutant in the RR genes are significantly less neurovirulent following intracranial injection into mice (5) and rats (30) and are less able to reactivate from ganglionic latency than wild-type virus (20). All cell culture work was carried out with Vero cells grown in Dulbecco's modified Eagle medium supplemented with 10% newborn calf serum.

Infection of ganglia and preparation of ganglionic extracts. Sprague-Dawley rats weighing 175 to 225 g were inoculated in both eyes with approximately 2×10^6 PFU of virus in a 1-μl volume following corneal scarification. For DNA and RNA analyses, the animals were sacrificed by decapitation, and the trigeminal ganglia were removed with sterile instruments and immediately transferred to a freezing solution. The single ganglia were homogenized in TRI reagent (Molecular Research Center Inc.), and DNA and RNA were extracted as instructed by the manufacturer. For histologic analyses, the ganglia were frozen in isopentane, embedded in OCT embedding medium (Miles Laboratory), and sectioned in a cryostat, or animals were perfused with 4% paraformaldehyde and the ganglia were embedded in paraffin and cut on a microtome. Both ganglia from two animals at each time point were individually examined by in situ hybridization and in situ PCR.

PCR amplification of DNA and RNA. DNA and RNA were amplified as previously described (30). The primers used were (i) for the glycoprotein B (*gB*) gene, ATT-CTC-CTC-CGA-CGC-CAT-ATC-CAC-CAC-CTT (5′ primer) and AGA-AAG-CCC-CCA-TTG-GCC-AGG-TAG-T (3′ primer); (ii) for the *lacZ* gene, TTG-CTG-ATT-CGA-GGG-GTT-AAC-CGT-CAC-GAG (5′ primer) and ACC-AGA-TGA-TCA-CAC-TGC-GGT-GAT-TAC-GAT (3′ primer) (13); (iii) for *LAT* genes, GAC-AGC-AAA-AAT-CCC-GTC-AG (5′ primer) and ACG-AGG-GAA-AAC-AAT-AAG-GG (3′ primer) (23); and (iv) for the glyceraldehyde phosphate dehydrogenase (*GAPDH*) gene, ATT-GGG-GGT-AGG-AAC-ACG-GAA (5′ primer) and ACC-CCT-TCA-TTG-ACC-TCA-ACT-A (3′ primer).

Samples were amplified in either a PTC 100 Programmable Thermal Controller (MJ Research Inc.) or a Bellco DNA Pacer (Bellco Biotechnology) for 30 cycles. For the *gB* and *lacZ* genes, the conditions were 95°C for 15 s, 54°C for 15 s, and 71°C for 1.5 min. For the *LAT* and *GAPDH* genes, amplification cycle conditions were 30 cycles at 95°C for 1 min and 60°C for 1 min, followed by a single extension at 72°C for 10 min. Reaction products were separated on 4% NuSieve agarose gels.

Competitive quantitative DNA PCR. The method used for competitive quantitative PCR has been described previously (30). We constructed a mutant template which is identical to a 191-bp fragment of the native HSV-1 *gB* gene except for a single base pair change creating a new *Hpa*II site 29 bases from the 3′ end. Known amounts of mutant template were added to each reaction tube, and following amplification, the products were digested with *Hpa*II. DNA fragments of 191 bp representing amplified wild-type *gB* sequences and 162 bp representing the amplified mutant sequences were electrophoretically separated, and the amount of *gB* DNA in the original sample was determined by comparison with the amount of amplified standard.

Ten microliters of DNA extract was coamplified with a 10-fold dilution series of the mutant *gB* fragment ranging from 10 pg to 1 fg for 30 cycles. To eliminate heterodimer formation (2, 15), the reaction products were diluted 200-fold and reamplified for two cycles in the presence of 1 μl of [α-^{32}P] dCTP (400 Ci/mmol; Amersham). The amplified products were digested with *Hpa*II, separated on a 4% NuSieve GTG agarose gel in 1× Tris-borate-EDTA buffer, and exposed to X-ray film (Hyperfilm-MP; Amersham). The approximate amount of *gB* DNA was determined by inspection of the autoradiograph. Ten-microliter aliquots of the ganglionic extract were then coamplified with a twofold serial dilution of mutant *gB* DNA ranging from 50 to 3.1 fg. Following *Hpa*II digestion and separation, the amount of radioactivity in each band was counted with a radioanalytic imaging detector (AMBIS Inc.). Standard linear regression curves were prepared by plotting net counts per minute for each sample in the dilution series against the amount of input mutant *gB* DNA, using the GraphPAD INPLOT software program (GraphPAD Software), and the amount of *gB* DNA was determined from the point of equivalence of the mutant and target products.

LAT DNA was quantitated in a similar manner. The normal *LAT* PCR product is 195 bp long, with a *Bsa*HI site 21 bp from the 3′ end. A mutant *LAT* DNA template, in which the *Bsa*HI site was removed as a consequence of a single base change (30), allowed the amplification products to be distinguished from one another following *Bsa*HI digestion; wild-type *LAT* fragments produced a 174-bp DNA, while the mutant template produced a 195-bp DNA.

Ten microliters of each extract was amplified by using primer pairs for the cellular *GAPDH* gene in the presence of [α-^{32}P]dCTP as a tracer, to ensure that the extracts contained equivalent amounts of DNA. The amounts were equivalent in each sample (data not shown), and no adjustment was necessary.

Competitive quantitative RT-PCR. The amount of LAT RNA in ganglia was determined by competitive quantitative RT-PCR, using a technique described previously (30). Mixtures of target and standard RNAs were reverse transcribed, and the resulting DNA templates were amplified in the presence of the wild-type *LAT* primers. The amplified DNA fragments were then processed as described for DNA quantitation. The standard RNA was prepared in a series of in vitro reactions (30).

Five microliters of extract was mixed with a 10-fold dilution series of mutant LAT RNA ranging from 1 μg to 1 fg and subjected to RT-PCR. The samples were amplified for 30 cycles and diluted 200-fold, and following reamplification for an additional two cycles in the presence of 1 μl of [α-^{32}P]dCTP (400 Ci/mmol; Amersham), the products were digested with 20 U of *Bsa*HI at 37°C overnight. Reaction products were electrophoresed in 4% NuSieve GTG agarose gels and exposed to X-ray film, from which visual estimates of target RNA quantities were made. Five-microliter samples of extract were then coamplified with a twofold serial dilution of mutant LAT RNA ranging from 50 to 3.1 fg, using the same procedures. PCR products were processed, radioactivity was quantitated with the AMBIS system, and the counts were analyzed by linear regression as described for the viral DNA determinations.

Ten-microliter aliquots of each RNA extract were amplified by RT-PCR using primer pairs for the *GAPDH* transcript. The reaction products were electrophoresed on 1% agarose gels, the gels were dried, and the amount of radioactivity per reaction product band was quantitated as described above. The amounts of RNA in the extracts were equivalent, and no adjustment in the sample was necessary.

In situ hybridization. Six-micrometer sections of infected trigeminal ganglia on glass slides were deparaffinized in xy-

lene, rehydrated through graded ethanols, rinsed with phosphate-buffered saline (PBS), treated with 1% HCl in PBS for 5 min, and then acetylated with acetic anhydride in triethanolamine for 20 min. After successive washes with 70, 80, and 90% ethanol, the sections were equilibrated in hybridization solution (50% formamide, 10% dextran, 2× SSC [1× SSC is 0.15 M NaCl plus 0.015 M sodium citrate], 0.01% single-stranded DNA, 0.01% tRNA, 0.02% sodium dodecyl sulfate) and hybridized overnight at 56°C in hybridization buffer with a digoxigenin-labeled riboprobe antisense to the *LAT* sequence from a plasmid containing the *Bam*HI B fragment of HSV-1 generously provided by Jerold Gordon of the University of Pittsburgh (16). Posthybridization, the slides were rinsed three times with 50% formamide–1× SSC at 56°C and twice with 1× SSC at room temperature. The bound digoxigenin-labeled probe was localized with an alkaline phosphatase-conjugated antidigoxigenin antibody (1:250; Boehringer-Mannheim) detected with 5-bromo-4-chloro-3-indolylphosphate toluidium–nitroblue tetrazolium (BCIP-NBT; Vector Laboratories).

In situ PCR. In situ PCR was carried out by using a modification of previously described methods (28, 38). Six-micrometer sections of infected trigeminal ganglia on glass slides were deparaffinized in xylene, successively rehydrated with graded ethanols, washed in PBS (pH 7.5) for 5 min, washed in 1% HCl in PBS for 5 min, and then washed in PBS for 3 h. The sections were rinsed in PCR buffer II (Perkin-Elmer), and 25 μl of PCR mixture (1× PCR buffer II, 1 mM $MgCl_2$, 1× digoxigenin DNA labeling mix, 100 ng of primer mix, 50% glycerol, 1 μl of *Taq* polymerase) was layered onto the sections, which were covered with a glass coverslip and sealed with nail polish, taking care to ensure that the polish did not seep into the reaction mix. PCR amplification was carried out in a BioOven II Thermal Cycler (BioTherm Corp.) in two stages: first for 3 cycles at 92°C for 1 min, 54°C for 30 s, and 72°C for 30 s, and then for 25 cycles at 92°C for 15 s, 54°C for 15 s, and 72°C for 15 s. After amplification, the coverslips were removed and the sections were washed successively with 1× SSC (twice for 5 min each time), 50% formamide in 1× SSC (three times for 15 min each time, 56°C), and 1× SSC (twice for 15 min each time). Following a rinse in Tris-buffered saline (pH 7.5) and 5% normal goat serum, the digoxigenin-labeled amplified DNA was localized by using an antidigoxigenin antibody conjugated to alkaline phosphatase (1:250; Boehringer Mannheim) and detected with BCIP-NBT (Vector Laboratories). Color development was monitored visually and stopped typically after about 30 min by washing with 0.1 M Tris-HCl (pH 7.5)–1 mM EDTA.

Southern hybridization. To confirm the specificity of the amplification products from both solution and in situ PCR amplification, samples were electrophoresed on agarose gels and transferred to a nylon membrane (GeneScreen Plus; NEN Research Products) by using a vacuum blotter (trans-Vac TE80; Hoefer Scientific Instruments). DNA was hybridized with γ-^{32}P-5′-end-labeled *gB* or *LAT* oligonucleotide DNA probes complementary to sequences internal to the primer sequences, using the Rapid-hyb buffer system (Amersham Life Sciences International) as directed by the manufacturer. Blots were exposed to X-ray film (Hyperfilm-MP; Amersham).

RESULTS

PCR analysis of viral DNA and RNA in infected rat trigeminal ganglia. Infection was initiated by the inoculation of 2 × 10^6 PFU of the RR1-RR2 mutant of HSV-1 (1 μl of a 2 × 10^9-PFU/ml stock) into each eye following corneal scarification. All infected animals survived the treatment. The persistence of viral genomes and transcripts in infected ganglia was detected by nonquantitative PCR amplification of ganglionic DNA and RNA. The *gB* and *LAT* DNA sequences served as representatives of the viral genome, while gB and LAT RNAs served to measure transcription of lytic cycle and latent cycle genes, respectively. The cellular *GAPDH* gene and message served as internal controls for nucleic acid isolation and amplification.

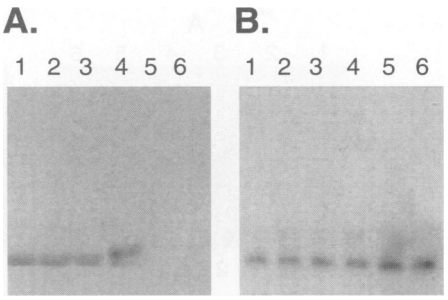

FIG. 1. PCR analysis of viral DNA and RNA in trigeminal extracts after corneal scarification and infection with the RR1*CAT*/RR2*lacZ* virus. PCR products were electrophoresed on a 1% agarose gel, Southern blotted, and hybridized with appropriate *gB* or *LAT* oligonucleotide probes. (A) Amplification of viral *gB* DNA and RNA, using *gB* primers. Lanes: 1 to 3, DNA amplification products from day 2, day 7, and week 8 infected trigeminal extracts respectively; 4 to 6, RNA amplification products from day 2, day 7, and week 8 infected trigeminal extracts, respectively. (B) Amplification of viral *LAT* DNA and RNA using *LAT* primers. Lanes: 1 to 3, DNA amplification products from day 2, day 7, and week 8 infected trigeminal extracts, respectively; 4 to 6, RNA amplification products from day 2, day 7, and week 8 infected trigeminal extracts, respectively, using *LAT* primers.

At 2 days, 7 days, and 8 weeks p.i., both *gB* (Fig. 1A, lanes 1 to 3) and *LAT* (Fig. 1B, lanes 1 to 3) DNAs were detected by amplification of DNA from extracts of ganglia of inoculated rats. No *gB* or *LAT* signals were evident in extracts of trigeminal ganglia from uninfected animals (data not shown). Both gB mRNA and LAT RNA were amplified from RNA extracted from 2-day-p.i. ganglia by using RT-PCR (Fig. 1A, lane 4; Fig. 1B, lane 4). In contrast, 7-day- and 8-week-p.i. ganglia contained no detectable gB RNA (Fig. 1A, lanes 5 and 6) even though *gB* DNA sequences were present in the same ganglia (lanes 2 and 3). LAT RNA, however, was amplified from the same extracts at 7 days and 8 weeks p.i. (Fig. 1B, lanes 5 and 6). No gB or LAT RNA signals were found when samples of the extract were treated with RNase before the start of the RT-PCR, demonstrating that the templates for RT-PCR were RNase sensitive. These results, showing that while RR1-RR2 mutant genomes transcribed both lytic cycle (gB) and latency (LAT) RNAs at 2 days p.i. but by 7 days expressed only LAT RNA in the absence of gB mRNA, suggest that HSV-1 latency was established in the trigeminal ganglia by 7 days. This characterization of the status of the viral genome as well as its expression in trigeminal ganglia correlates with the findings of our previous study on the establishment of latency in the rat brain (30).

Quantitation of viral DNA and RNA in trigeminal ganglia. The amounts of viral DNA and LAT RNA in the trigeminal ganglia were quantitated by competitive quantitative PCR and RT-PCR. Five infected rats at each time point were sacrificed, and both trigeminal ganglia from the same animal were

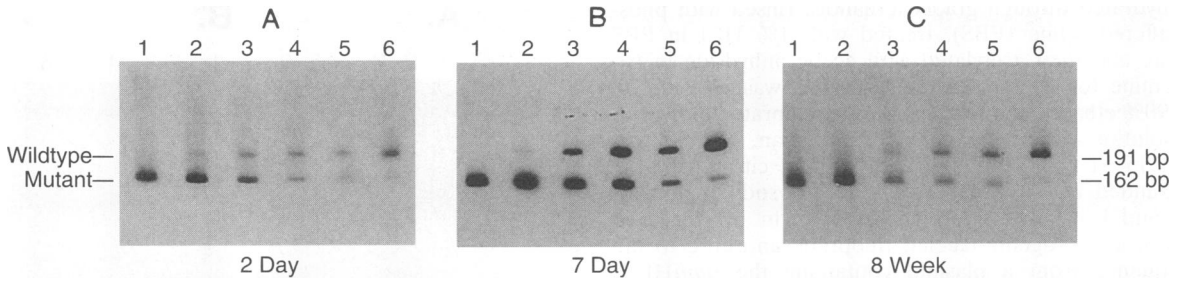

FIG. 2. Competitive quantitative *gB* DNA PCR. DNAs from infected rat trigeminal extracts were coamplified with a twofold dilution series of competitor mutant *gB* DNA, using *gB* primers. Radioactive PCR products were digested with *Hpa*II and electrophoresed on 4% NuSieve GTG agarose gels. Gels were dried and exposed to X-ray film, and radioactivity was quantitated by analyzing dry gels with the AMBIS system. A representative autoradiograph is shown. (A) Lanes: 1, 100 fg of mutant *gB* DNA coamplified with a day 2 uninfected trigeminal extract; 2 to 6, twofold dilution series of mutant *gB* DNA, ranging from 100 fg (lane 2) to 6.25 fg (lane 6), coamplified with day 2 infected trigeminal extracts. (B) Lanes: 1, 100 fg of mutant *gB* DNA coamplified with a day 7 uninfected trigeminal extract; 2 to 6, twofold dilution series of mutant gB DNA, ranging from 100 fg (lane 2) to 6.25 fg (lane 6), coamplified with day 7 infected trigeminal extracts. (C) Lanes: 1, 100 fg of mutant *gB* DNA coamplified with a week 8 uninfected trigeminal extract; 2 to 6, twofold dilution series of mutant *gB* DNA, ranging from 100 fg (lane 2) to 6.25 fg (lane 6), coamplified with week 8 infected trigeminal extracts.

processed together and assayed, in triplicate for each extract. Representative data for trigeminal ganglia amplified for *gB* DNA at each time point are shown in Fig. 2. The upper bands represent the wild-type 191-bp amplified product of the viral *gB* DNA in the trigeminal ganglia extracts, while the lower bands represent the *Hpa*II-digested 162-bp fragment derived from the 191-bp mutant competitor DNA. The observed decrease in radioactivity reflects the twofold dilution of the mutant *gB* template, which is linear (data not shown). The results of linear regression analyses of the average net counts per minute of ^{32}P detected in each band for five animals, each ascertained from three independent measurements at each time point, are summarized in Table 1. The amount of *gB* DNA in the trigeminal ganglia remained relatively constant: 40.9, 44.1, and 46.4 fg for 2 days, 7 days, and 8 weeks p.i., respectively. These values correspond to 1.9×10^5 genome equivalents per trigeminal ganglion at 2 days, 2.1×10^5 at 7 days, and 2.2×10^5 at 8 weeks.

Competitive quantitative PCR analysis of *LAT* DNA yielded values that were consistent with the *gB* determinations. There were 83.7 fg of *LAT* DNA per ganglion at 2 days, 90.1 fg at 7 days, and 83.9 fg at 8 weeks p.i. (Table 1). The ratios of *LAT* DNA to *gB* DNA, 2.04, 2.05, and 1.81 for 2 days, 7 days, and 8 weeks p.i., respectively (Table 1), reflect the fact that there are two copies of the *LAT* gene but only one copy of the *gB* gene in each HSV-1 genome. The capacity to detect twofold differences attests to the sensitivity and accuracy of the competitive quantitative PCR technique. Like the amount of *gB* DNA, the amount of *LAT* DNA remained relatively constant between 2 days and 8 weeks p.i.

The amount of LAT RNA was determined by competitive quantitative RT-PCR. Figure 3 presents representative amplification results for both trigeminal ganglia excised from single animals sacrificed on 2 days, 7 days, and 8 weeks p.i. The upper set of bands represent the twofold dilution series of the 195-bp mutant standard RNA, ranging from 100 to 6.25 fg, while the lower bands represent the 174-bp amplified target DNA after *Bsa*HI digestion. The average amounts of LAT RNA per ganglion were 2.0 pg at 2 days, 2.2 pg at 7 days, and 2.9 pg at 8 weeks p.i., corresponding to 9.7×10^6, 1.0×10^7, and 1.4×10^7 LAT RNA molecules per ganglion, respectively, at those time points (Table 1). It appears that the number of LAT RNA molecules remained relatively constant between 2 and 7 days and may have increased slightly by 8 weeks, although that difference is not statistically significant. We estimate that there were 50 to 60 LAT molecules per HSV-1 genome on the average (Table 1).

No amplification was observed when aliquots from each extract were pretreated with RNase prior to the reaction, confirming that the RT-PCR exclusively amplified RNA (Fig. 3, lanes 1). In addition, there was no amplification when the Moloney murine leukemia virus reverse transcriptase was not

TABLE 1. Quantitation of genome equivalents of HSV-1 and LAT RNAs in the rat trigeminal ganglion

Time p.i.	Amt of *gB* DNA (fg)[a]	No. of genome equivalents[b] (10^5)	Amt of *LAT* DNA (fg)[a]	Ratio of *LAT* DNA to *gB* DNA	Amt of LAT RNA (pg)[c]	No. of LAT RNA molecules[d]	No. of LAT RNA molecules/genome equivalent
2 days	40.9 ± 1.9	1.9	83.7 ± 7.2	2.04	2.0 ± 0.2	9.7×10^6	51.1
7 days	44.1 ± 4.5	2.1	90.1 ± 6.6	2.05	2.2 ± 0.2	1.0×10^7	47.6
8 weeks	46.4 ± 5.1	2.2	83.9 ± 1.8	1.81	2.9 ± 0.3	1.4×10^7	63.6

[a] Net counts per minute corresponding to amplified wild-type and mutant *gB* or *LAT* DNA were quantified by using the AMBIS radioanalytic imaging system, and the amounts of wild-type *gB* DNA were determined from linear regression plots of net counts per minute against amounts of input mutant DNA. Each value shown is an average from five different animals, each measured from three independent sections, ± standard deviation. The larger amount of *LAT* DNA reflects the diploid nature of the *LAT* gene in the HSV-1 genome.

[b] The *gB* PCR product is 191 bp, which corresponds to 1.26×10^5 g/mol. The total number of gB molecules was calculated by using Avogadro's number. Since *gB* is a single-copy gene, the number of gB molecules is also the number of genome equivalents.

[c] The amount of LAT RNA was calculated in a manner similar to that for *gB* DNA, by using linear regression plots of net counts per minute against amounts of input mutant LAT RNA. Each value shown is an average from five different animals, each measured from three independent sections, ± standard deviation.

[d] The *LAT* PCR product is 195 bp, corresponding to 1.28×10^5 g/mol. As in the case of *gB*, the total number of LAT RNA molecules was calculated from Avogadro's number.

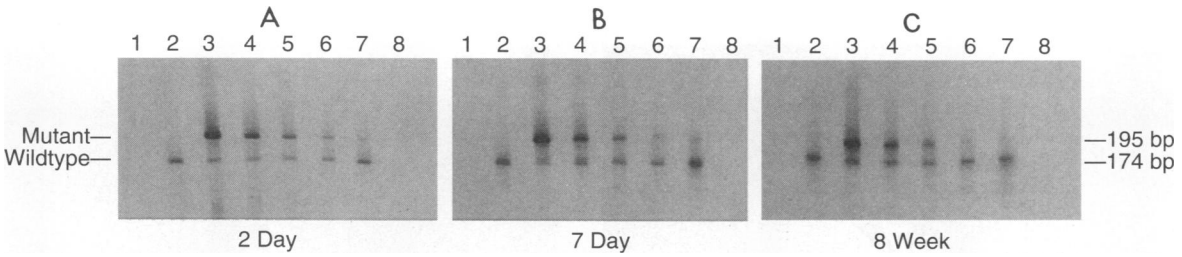

FIG. 3. Competitive quantitative RT-PCR of LAT RNA. RNAs from infected trigeminal ganglia were reverse transcribed and coamplified with a twofold dilution series of competitor mutant LAT RNA as described in the text. Radioactive RT-PCR products were digested with *Bsa*HI and electrophoresed on 4% NuSieve GTG agarose gels. Gels were dried and exposed to X-ray film. Radioactivity was quantitated by analyzing dried gels with the AMBIS system. A representative autoradiograph is shown. (A) Lanes: 1, RT-PCR products from day 2 infected trigeminal extract after RNase treatment; 2, RT-PCR products from day 2 infected trigeminal extract; 3 to 7, RT-PCR products from a twofold dilution series of mutant LAT RNA, ranging from 50 fg (lane 3) to 3.1 fg (lane 7), added to day 2 infected trigeminal extracts; 8, RT-PCR products from day 2 infected trigeminal extract without addition of reverse transcriptase. (B) Lanes: 1, RT-PCR products from day 7 infected trigeminal extract after RNase treatment; 2, RT-PCR products from day 7 infected trigeminal extracts; 3 to 7, RT-PCR products from a twofold dilution series of mutant LAT RNA, ranging from 50 fg (lane 3) to 3.1 fg (lane 7), added to day 7 infected trigeminal extract; 8, RT-PCR products from day 7 infected trigeminal extracts without addition of reverse transcriptase. (C) Lanes: 1, RT-PCR products from week 8 infected trigeminal extract after RNase treatment; 2, RT-PCR products from week 8 infected trigeminal extract; 3 to 7, RT-PCR products from a twofold dilution series of mutant LAT RNA, ranging from 50 fg (lane 3) to 3.1 fg (lane 7), added to week 8 infected trigeminal extracts; 8, RT-PCR products from week 8 infected trigeminal extracts without addition of reverse transcriptase.

added to the untreated reaction mixture (Fig. 3A, lane 8; Fig. 3B, lane 8; Fig. 3C, lane 7). To confirm that the restriction digestions were complete after the PCR, extracts in the absence of any standard competitor RNA were amplified and restriction enzyme digested, resulting in a single product of 174 bp (Fig. 3A, lane 2; Fig. 3B, lane 2; Fig. 3C, lane 2).

Identification of neurons expressing LAT RNA. Six animals were inoculated in each eye, and at each time point (2 days, 7 days, and 8 weeks), two animals were sacrificed and the four trigeminal ganglia were individually processed for analysis by in situ hybridization. The distribution of ganglion cells expressing LAT RNA was determined by in situ hybridization with a digoxigenin-labeled riboprobe antisense to the LAT RNA sequence. Every 5th slide (containing four 6-μm sections per slide) or every 10th slide (containing two 6-μm sections) was examined. Every ganglion had LAT-positive cells, although many sections contained no LAT-positive cells. The number of positive cells in the ganglia were generally few, although there is a suggestion that the 2-day ganglia may have more than the 7-day and 8-week tissues (Table 2). The sections from the 7-day and 8-week ganglia which showed LAT-positive cells typically contained only one to two positive cells per section (Fig. 4A and B; Table 2), and the maximum number of LAT-expressing cells seen in any single section was five. These data are consistent with previous reports of in situ hybridization studies of LAT expression in latently infected trigeminal ganglia (6, 20, 33, 34). We estimate that there were approximately 10 to 20 LAT-positive cells per ganglion at 7 days and 8 weeks, although we did not perform in situ hybridization on serial sections through the ganglion.

In situ PCR. To determine whether viral genomes in the ganglion were restricted to the LAT-positive neurons detected by in situ hybridization, we examined selected sections from the same ganglion by in situ PCR to detect HSV-1 DNA. *gB* primers and digoxigenin-labeled nucleotides were used to produce digoxigenin-labeled DNAs in situ, which were then localized by using an alkaline phosphatase-conjugated anti-digoxigen antibody detected with the BCIP-NBT substrate. In contrast to in situ hybridization which detects LAT RNA, in situ PCR detection of viral DNA showed many positive cells in every section chosen because of their proximity to LAT-positive sections. The signals, localized to neuronal cells, were nuclear in location and varied in intensity (Fig. 4C and D). The number of positive neurons in sections (at least 10 sections from each animal) from all 12 ganglia were counted. The maximum number of HSV-1 DNA-positive cells in the ganglia ranged from 29 to 120 per section. The data in Table 2 presents the distribution of the maximum number of *gB* DNA in situ PCR-positive cells observed in the 12 infected ganglia.

A number of controls were performed to determine that the in situ PCR results were specific for the HSV-1 *gB* gene sequence. (i) In situ PCR using *gB* primers and uninfected ganglia failed to show any labeled nuclei (Fig. 4E). (ii) No in situ signals were detected in infected ganglia, using a primer pair for the HIV *tat* gene not present in the tissue (Fig. 4F). (iii) DNase treatment of sections from infected animals prior to PCR eliminated the PCR signals (Fig. 4G). (iv) Finally, DNA extracted from sections of infected ganglia after PCR was completed hybridized to *gB*-specific probes in Southern blot analyses. Single radioactive bands of the expected length were observed (Fig. 5).

TABLE 2. Maximum number of in situ hybridization and in situ PCR-positive neurons per section in the HSV-1 latent trigeminal ganglia[a]

Assay	No. of positive neurons					
	2 days p.i.		7 days p.i.		8 wk p.i.	
	Left	Right	Left	Right	Left	Right
In situ hybridization for LAT RNA	5	4	3	3	5	5
	29	8	3	5	3	4
In situ PCR for *gB* DNA	54	91	52	51	31	46
	59	116	29	73	62	120

[a] Six rats were each inoculated with 2×10^6 PFU virus in a 1-μl volume following corneal scarification. At each time point, two animals were sacrificed, all trigeminal ganglia were excised, and 6-μm sections were processed for in situ hybridization and in situ PCR as described in the text. At least 10 sections from each of the 12 infected ganglia were examined for hybridization and for PCR-positive cells.

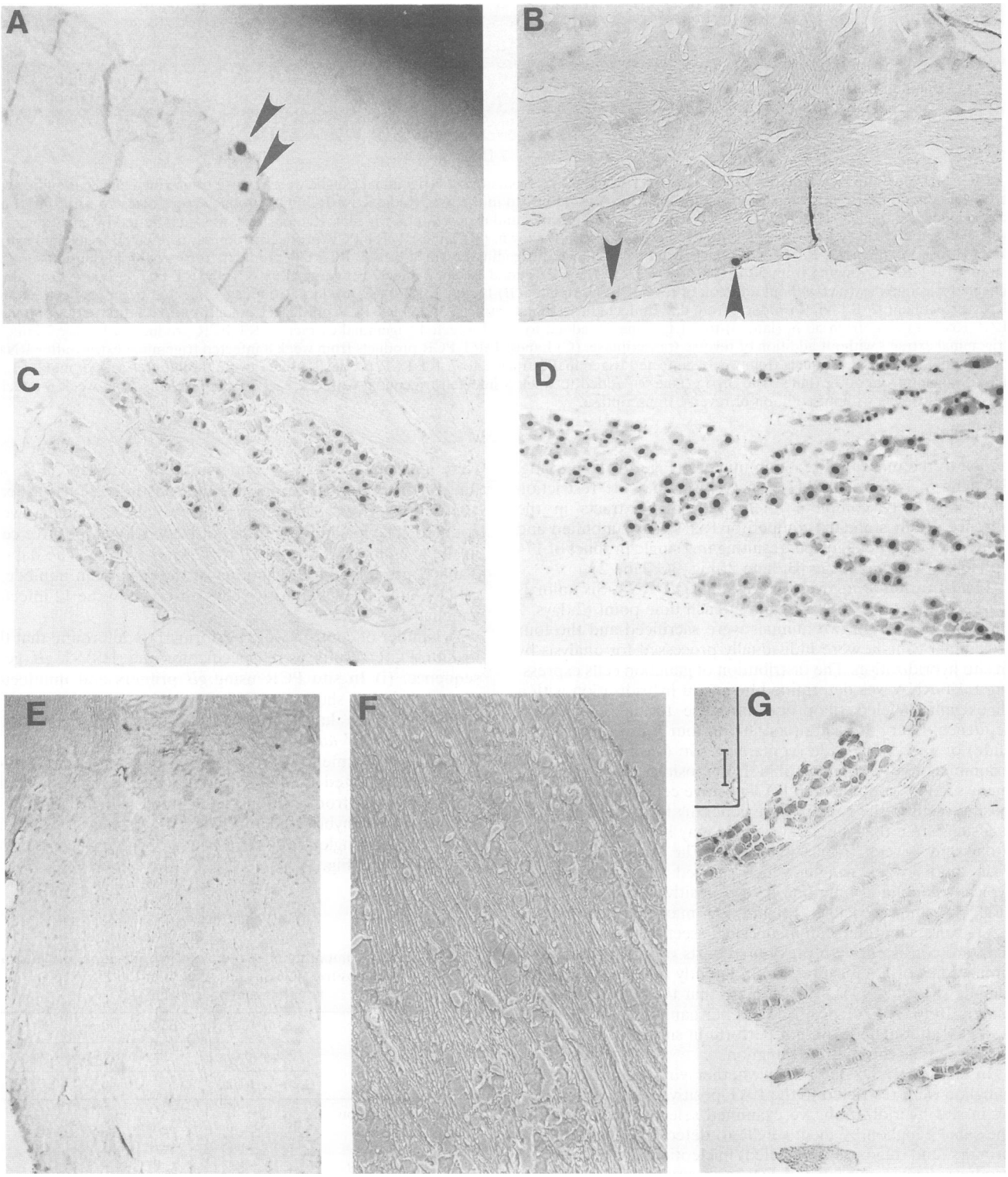

FIG. 4. In situ detection of HSV-1 DNA and RNA in trigeminal ganglia. (A and B) In situ hybridization of trigeminal ganglion with a digoxigenin-labeled riboprobe for HSV-1 LAT at 7 days (A) and 8 weeks (B) p.i. Arrowheads point to positive cells. (C and D) In situ PCR of parallel sections with oligonucleotide primers for HSV-1 *gB* DNA sequences and digoxigenin-labeled nucleotides at 7 days (C) and 8 weeks (D) p.i. Controls: (E) Uninfected ganglion, amplified with primers for the HSV-1 *gB* gene; (F) 8-week-p.i. ganglion amplified with primers for HIV *tat*; (G) 8-week-p.i. ganglion, amplified with primers for HSV-1 *gB* gene after overnight DNase I treatment. Bar, 100 μm.

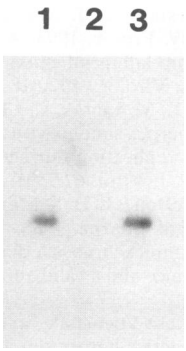

FIG. 5. Southern hybridization of DNA extracted off single 6-μm sections after in situ PCR using *gB* primers. Extracted DNA was electrophoresed on a 1% agarose gel in 1× Tris-borate-EDTA buffer, transferred to a GeneScreen Plus membrane, and hybridized with an internal ^{32}P-labeled *gB* oligonucleotide probe. Lanes: 1, DNA from a week 8 infected ganglionic section after amplification; 2, DNA from an uninfected ganglionic section after amplification; 3, control 191-bp *gB* fragment.

DISCUSSION

The data presented in this report offer important new information in the consideration of the biology of HSV-1 latency in peripheral ganglia. We have obtained specific quantitation of the number of genomes which persist in the trigeminal ganglion and the number of LATs in the ganglion during latency and have defined the relationship of HSV-1 genome-bearing cells to LAT RNA-containing cells in the ganglion. PCR demonstration of persistent HSV-1 genomes, with RT-PCR demonstration of LAT RNA but not gB mRNA at 7 days and 8 weeks p.i., shows that the RR-defective attenuated mutant virus established a latent state in these neurons. Although we have not directly demonstrated the absence of replicating virus or reactivation of virus from these ganglia, it is likely that the viral genomes are latent because of the absence of lytic gene expression.

Competitive quantitative PCR established that there were approximately 2×10^5 genome equivalents per ganglion at 2 days, 7 days, and 8 weeks p.i. Each eye had been inoculated with 2×10^6 PFU, and the RR1*CAT*/RR2*lacZ* viral stock contains 90 genome equivalents for each PFU (30), so that each eye received approximately 1.8×10^8 genomes. The recovery of 2×10^5 genome equivalents per ganglion represents 1 inoculated genome in 1,000 that established latency in the trigeminal ganglion under the conditions of the experiments. The similarity in amounts of viral DNA at 2 days and 7 days is consistent with the absence of viral replication in the ganglion. These data are in accord with evidence from others that RR-defective mutants do not produce infectious virus in trigeminal ganglia (20). Using another RR1 deletion mutant virus and a noncompetitive quantitative PCR technique, Katz et al. (21) found 10^4 genome equivalents per trigeminal ganglion in the mouse.

The amount of LAT RNA detected by RT-PCR was stable in the trigeminal ganglion over 8 weeks p.i., with 9.7×10^6 molecules per ganglion at 2 days, 1×10^7 molecules per ganglion at 7 days, and 1.4×10^7 molecules per ganglion at 8 weeks. In contrast to the central nervous system, where we found approximately 15 LAT molecules per genome during latency (30), this represents 51.1, 47.6, and 63.6 LAT molecules per genome in the trigeminal ganglion at the three respective time points. The amount of LAT molecules is maintained, and there is no evidence for loss of transcripts over 8 weeks. Taking both the DNA and RNA data into account, we conclude that once latency is established in the trigeminal ganglion, there is no significant loss of template or transcript over 8 weeks, and presumably for the life of the host.

The number of genomes which have been previously reported to persist in latently infected trigeminal ganglia varies widely. Using wild-type KOS and a mouse model, Rodahl and Stevens (33) found 3,500 genomes in trigeminal ganglion at 21 days p.i. In contrast, Cai et al. (4) estimated that there were 500 to 50,000 genomes persisting in their model. Katz et al. (21) estimated 5×10^5 genomes, and Sawtell and Thompson (35) measured 1.2×10^6 to 3.6×10^7 genomes per trigeminal ganglion during latency. Although our model differs in species (Sprague-Dawley rats versus various mouse strains), in the use of a deletion mutant compared with wild-type KOS, and in our use of a competitive instead of a noncompetitive PCR assay, our value of approximately 2×10^5 genomes per trigeminal ganglion is well within the range reported by other workers.

The number of LAT-positive cells which we detected per ganglion is also within the range of estimates obtained by others using different model systems. Jacobson et al. (20) found 12 LAT-positive cells in each tissue section after establishing latency in the trigeminal ganglion with wild-type KOS but only 2.5 LAT-positive cells per section when latency was established with a thymidine kinase-deficient (TK^-) mutant, which like our RR^- mutant is replication defective in neurons. Coen et al. (6) similarly found 8 LAT-positive cells per section of trigeminal ganglion after inoculation with wild-type KOS but only 1.5 to 2.5 LAT-positive cells per section after inoculation with a TK^- mutant. Sawtell and Thompson (35) averaged 31 detected cells (using a *lacZ* reporter gene driven by the LAT promoter) in latent ganglia in their model. Only Rodahl and Stevens (33) found a high number of LAT-positive cells (340), but they used anterior chamber inoculation rather than the corneal scarification used in our study. In this context, the presence of one to five LAT-positive cells per section that we detected in latent ganglia appears to conform to previous reports.

While previous estimates of the number of HSV-1 genomes per cell during latency in the mouse trigeminal ganglion have ranged from 0.3 to 3 (21, 35), these values are based on the total number of cells in the ganglion, a number which includes satellite cells. Because HSV-1 establishes latency in neurons, the actual number of genomes in each cell that contains HSV genomes must be substantially higher than those earlier estimates. Sawtell and Thompson (35) calculated 3×10^4 to 1×10^6 genomes for each LAT-positive cell in their model. The in situ PCR, however, demonstrates that a large proportion of HSV genome-bearing neurons in the trigeminal ganglion do not express detectable LATs. We found as many as 120 neurons harboring viral genomes by in situ PCR in a single section, and the number of positive cells per section detected by in situ PCR was at least 10-fold and sometimes 50-fold greater than the number of LAT-positive cells per section detected by in situ hybridization from the same ganglia. A similar discordance was reported by Gressens and Martin (17) in the mouse trigeminal ganglion and brain latently infected with wild-type HSV-2; they also used in situ PCR to detect viral DNA and in situ hybridization for detection of LAT RNA-expressing neurons. The rodent trigeminal ganglion contains only about 20,000 neurons, of which 250 to 400 project to the cornea (1, 24). Thus, the number of genome-containing neurons in our model is of the same order of magnitude as the number of neurons in the ganglion that project to the cornea, and consequently the number of HSV-1 genomes per positive

cell must be considerably less than that calculated for LAT-positive cells. We are currently carrying out a double-label tracing study to determine whether all of those neurons contain HSV-1 genomes and whether HSV-1 genomes are restricted to neurons projecting directly to the cornea.

How can the apparent disproportion between the number of HSV-1 genome-bearing neurons and the number of LAT-positive cells be understood? One explanation is that while all latent HSV-1 genomes produce similar amounts of LAT RNA (calculated at approximately 50 LATs per genome by competitive quantitative PCR), those genomes are heterogeneously distributed, with many cells containing few genomes and isolated cells containing many genomes. In this case, all the neurons harboring any viral genomes would produce LAT RNA, but since only those nuclei containing at least a threshold level appear as LAT positive by in situ hybridization, only a few positive cells are detected. It is not immediately apparent how the development of such a heterogeneous distribution of HSV genomes might be explained. In situ RT-PCR might establish that there is a wider distribution of LAT-positive cells than can be detected by in situ hybridization. A second possible explanation is that the genomes are relatively homogeneously distributed throughout neurons in the ganglion, but that only some of these genomes are producing LATs. In this case, the average number of LATs per genome calculated by competitive quantitative PCR could not be extrapolated to apply to all genomes. Neurons in the trigeminal ganglion can be classified by differential gene expression of neurotransmitters, growth factor receptors, and other phenotypic markers (25). Specific cellular factors may be required to transactivate LAT expression, which would then occur in only a restricted subset of the ganglionic neurons harboring latent viral genomes. If this is indeed the case, then there would be 5×10^5 LAT molecules per LAT-positive cell in our experimental system. The occurrence of cells which harbor viral genomes but which do not appear to contain LAT RNA would support the contention that LAT expression is not a requirement for the establishment or maintenance of the latent state, an idea that is also supported by the observation that LAT-deleted mutant viruses are able to establish latency (19, 36, 39).

These observations also have implications for the potential use of HSV-1 as a gene transfer vector for the nervous system. The presence of latent viral genomes in a large number of cells suggests that HSV-1 may be more efficient in establishing the latent state, that is, establishing latency in a higher proportion of neurons, than would be anticipated from previously reported data. However, the paucity of LAT expression suggests that alternative strategies for driving gene expression may need to be developed in order to fully exploit those genomes which persist in the nervous system as a platform for gene expression.

ACKNOWLEDGMENTS

We thank Guihua Jiang for help with the in situ hybridization experiments and histology.

This work was supported by Public Health Service grants R01AI8228 from the National Institute of Allergy and Infectious Diseases and R01AG09470 from the National Institute of Aging and by a grant from the Veterans Administration.

REFERENCES

1. **Arvidson, B.** 1977. Retrograde axonal transport of horseradish peroxidase from cornea to trigeminal ganglion. Acta Neuropathol. **38**:49–52.
2. **Becker-Andre, M., and K. Hahlbrock.** 1989. Absolute mRNA quantitation using the polymerase chain reaction (PCR). A novel approach by a PCR aided transcript titration assay (PATTY). Nucleic Acids Res. **17**:9437–9446.
3. **Block, T. M., S. Deshmane, J. Masonis, J. Maggioncalda, T. Valyi-Nagi, and N. W. Fraser.** 1993. An HSV LAT null mutant reactivates slowly from latent infection and makes small plaques on CV-1 monolayers. Virology **192**:618–620.
4. **Cai, W., T. L. Astor, L. M. Liptak, C. Cho, D. M. Coen, and P. A. Schaffer.** 1993. The herpes simplex virus type 1 regulatory protein ICP0 enhances virus replication during acute infection and reactivation from latency. J. Virol. **67**:7501–7512.
5. **Cameron, J. M., I. McDougall, H. S. Marsdan, V. G. Preston, D. J. Ryan, and J. H. Subak-Sharpe.** 1988. Ribonucleotide reductase encoded by herpes simplex virus is a determinant of the pathogenicity of the virus in mice and a valid antiviral target. J. Gen. Virol. **69**:2607–2612.
6. **Coen, D. M., M. Kosz-Vnenchak, and J. G. Jacobsen.** 1989. Thymidine kinase-negative herpes simplex virus mutants establish latency in mouse trigeminal ganglia but do not reactivate. Proc. Natl. Acad. Sci. USA **86**:4736–4740.
7. **Deatly, A. M., J. G. Spivack, E. Lavi, D. R. O'Boyle II, and N. W. Fraser.** 1988. Latent herpes simplex virus type 1 transcripts in peripheral and central nervous system tissues of mice map to similar regions of the viral genome. J. Virol. **62**:749–756.
8. **Desai, P., R. Ramakrishnan, Z. W. Lin, B. Osak, J. C. Glorioso, and M. Levine.** 1993. The RR1 gene of herpes simplex virus type 1 is uniquely *trans* activated by ICP0 during infection. J. Virol. **67**:6125–6135.
9. **Deshmane, S. L., and N. W. Fraser.** 1989. During latency, herpes simplex virus type 1 DNA is associated with nucleosomes in a chromatin structure. J. Virol. **63**:943–947.
10. **Deshmane, S. L., M. Nicosia, T. Valyi-Nagy, L. T. Feldman, A. Dillner, and N. W. Fraser.** 1993. An HSV-1 mutant lacking the LAT TATA element reactivates normally in explant cocultivation. Virology **196**:868–872.
11. **Devi-Rao, G. B., S. A. Goodart, L. M. Hecht, R. Rochford, M. K. Rice, and E. K. Wagner.** 1991. Relationship between polyadenylated and nonpolyadenylated herpes simplex virus type 1 latency-associated transcripts. J. Virol. **65**:2179–2190.
12. **Efstathiou, S., A. C. Minson, H. J. Field, J. R. Anderson, and P. Wildy.** 1986. Detection of herpes simplex virus-specific DNA sequences in latently infected mice and in humans. J. Virol. **57**:446–455.
13. **Fink, D. J., L. R. Sternberg, P. C. Weber, M. Mata, W. F. Goins, and J. C. Glorioso.** 1992. *In vivo* expression of β-galactosidase in hippocampal neurons by HSV-mediated gene transfer. Hum. Gene Ther. **3**:11–19.
14. **Fraser, N. W., T. M. Block, and J. G. Spivack.** 1992. The latency-associated transcripts of herpes simplex virus: RNA in search of function. Virology **191**:1–8.
15. **Gilliland, G., S. Perrin, and H. F. Bunn.** 1990. Competitive PCR for quantitation of mRNA, p. 60–69. *In* M. A. Innis, D. H. Gelfand, J. J. Sninsky, and T. J. White (ed.), PCR protocols: a guide to methods and applications. Academic Press, New York.
16. **Gordon, Y. J., B. Johnson, E. Romanowski, and T. Araullo-Cruz.** 1988. RNA complementary to herpes simplex virus type I ICP0 gene demonstrated in neurons of human trigeminal ganglia. J. Virol. **62**:1832–1835.
17. **Gressens, P., and J. R. Martin.** 1994. *In situ* polymerase chain reaction: localization of HSV-2 DNA sequences in infections of the nervous system. J. Virol. Methods **46**:61–83.
18. **Hill, T. J.** 1985. Herpes simplex virus latency, p. 175–240. *In* B. Roizman (ed.), The herpesviruses. Plenum Press, New York.
19. **Ho, D. Y., and E. S. Mocarski.** 1989. Herpes simplex virus latent RNA (LAT) is not required for latent infection in the mouse. Proc. Natl. Acad. Sci. USA **86**:7596–7600.
20. **Jacobson, J. G., D. A. Leib, D. J. Goldstein, C. L. Bogard, P. A. Schaffer, S. K. Weller, and D. M. Coen.** 1989. A herpes virus ribonucleotide reductase deletion mutant is defective for productive acute and reactivable latent infections of mice and for replication in mouse cells. Virology **173**:276–283.
21. **Katz, J. P., E. T. Bodin, and D. M. Coen.** 1990. Quantitative polymerase chain reaction analysis of herpes simplex virus DNA in ganglia of mice infected with replication-incompetent mutants. J. Virol. **64**:4288–4295.
22. **Leib, D. A., C. L. Bogard, M. Kosz-Vnenchak, K. A. Hicks, D. M.**

Coen, D. M. Knipe, and P. A. Schaffer. 1989. A deletion mutant of the latency-associated transcript of herpes simplex virus type 1 reactivates from the latent state with reduced frequency. J. Virol. **63:**2893–2900.

23. **Lynas, C., K. A. Laycock, S. D. Cook, T. J. Hill, W. A. Blyth, and N. J. Maitland.** 1989. Detection of herpes simplex virus type 1 gene expression in latently and productively infected mouse ganglia using the polymerase chain reaction. J. Gen. Virol. **70:** 2345–2355.
24. **Marfurt, C. F., R. E. Kingsley, and S. E. Echtenkamp.** 1989. Sensory and sympathetic innervation of the mammalian cornea. Invest. Ophthalmol. Visual Sci. **30:**461–472.
25. **Margolis, T. P., C. R. Dawson, and J. H. LaVail.** 1992. Herpes simplex viral infection of the mouse trigeminal ganglion. Invest. Ophthalmol. Visual Sci. **33:**259–267.
26. **Mellerick, D. M., and N. W. Fraser.** 1987. Physical state of the latent herpes simplex virus genome in a mouse model system: evidence suggesting an episomal state. Virology **158:**265–275.
27. **Mitchell, W. J., R. P. Lirette, and N. W. Fraser.** 1990. Mapping of low abundance latency-associated RNA in trigeminal ganglia of mice latently infected with herpes simplex virus type 1. J. Gen. Virol. **71:**125–132.
28. **Nuovo, G. J.** 1992. PCR *in situ* hybridization: protocols and applications. Raven Press, New York.
29. **Puga, A., and A. L. Notkins.** 1987. Continued expression of a poly(A)$^+$ transcript of herpes simplex virus type 1 in trigeminal ganglia of latently infected mice. J. Virol. **61:**1700–1703.
30. **Ramakrishan, R., D. J. Fink, G. Jiang, P. Desai, J. C. Glorioso, and M. Levine.** 1994. Competitive quantitative PCR analysis of herpes simplex virus type 1 DNA and latency-associated transcript RNA in latently infected cells of the rat brain. J. Virol. **68:**1864–1873.
31. **Rock, D. L., and N. W. Fraser.** 1983. Detection of HSV-1 genome in central nervous system of latently infected mice. Nature (London) **302:**523–525.
32. **Rock, D. L., A. B. Nesburn, H. Ghiasi, J. Ong, T. L. Lewis, J. R. Lokensgard, and S. Wechsler.** 1987. Detection of latency-related viral RNAs in trigeminal ganglia of rabbits latently infected with herpes simplex virus type 1. J. Virol. **61:**3820–3826.
33. **Rodahl, E., and J. G. Stevens.** 1992. Differential accumulation of herpes simplex virus type 1 latency-associated transcripts in sensory and autonomic ganglia. Virology **189:**385–388.
34. **Roizman, B., and A. E. Sears.** 1987. An inquiry into the mechanisms of herpes simplex virus latency. Annu. Rev. Microbiol. **41:** 543–571.
35. **Sawtell, N. M., and R. L. Thompson.** 1992. Herpes simplex virus type 1 latency-associated transcription unit promotes anatomical site-dependent establishment and reactivation from latency. J. Virol. **66:**2157–2169.
36. **Sedarati, F., K. M. Izumi, E. K. Wagner, and J. G. Stevens.** 1989. Herpes simplex virus type 1 latency-associated transcription plays no role in establishment or maintenance of a latent infection in murine sensory neurons. J. Virol. **63:**4455–4458.
37. **Spivack, J. G., and N. W. Fraser.** 1987. Detection of herpes simplex virus type 1 transcripts during latent infection in mice. J. Virol. **61:**3841–3847.
38. **Staskus, K. A., L. Couch, P. Bitterman, E. F. Retzel, M. Zupancic, J. List, and A. T. Haase.** 1991. *In situ* amplification of visna virus DNA in tissue sections reveals a reservoir of latently infected cells. Microb. Pathog. **11:**67–76.
39. **Steiner, I., J. G. Spivack, R. P. Lirette, S. M. Brown, A. R. MacLean, J. Subak-Sharpe, and N. W. Fraser.** 1989. Herpes simplex virus type 1 latency-associated transcripts are evidently not essential for latent infection. EMBO J. **8:**505–511.
40. **Stevens, J. G.** 1989. Human herpesviruses: a consideration of the latent state. Microbiol. Rev. **53:**318–332.
41. **Stevens, J. G., and M. L. Cook.** 1971. Latent herpes simplex virus in spinal ganglia of mice. Science **173:**843–845.
42. **Stevens, J. G., E. K. Wagner, G. B. Devi-Rao, M. L. Cook, and L. T. Feldman.** 1987. RNA complementary to a herpesvirus gene mRNA is prominent in latently infected neurons. Science **235:** 1056–1059.
43. **Wagner, E. K., G. Devi-Rao, L. T. Feldman, A. T. Dobson, Y.-F. Zhang, W. M. Flanagan, and J. G. Stevens.** 1988. Physical characterization of the herpes simplex virus latency-associated transcript in neurons. J. Virol. **62:**1194–1202.
44. **Wagner, E. K., W. M. Flanagan, G. Devi-Rao, Y.-F. Zhang, J. M. Hill, K. P. Anderson, and J. G. Stevens.** 1988. The herpes simplex virus latency-associated transcript is spliced during the latent phase of infection. J. Virol. **62:**4577–4585.
45. **Wechsler, S. L., A. B. Nesburn, R. Watson, S. M. Slanina, and H. Ghiasi.** 1988. Fine mapping of the latency-related gene of herpes simplex virus type 1: alternative splicing produces distinct latency-related RNAs containing open reading frames. J. Virol. **62:**4051–4058.